RESEARCH ARTICLE

Journal of
Applied**Toxicology** WILEY

Proteomic analysis using isobaric tags for relative and absolute quantification technology reveals mechanisms of toxic effects of tris (1,3-dichloro-2-propyl) phosphate on RAW264.7 macrophage cells

Wei Zhang[1] [ORCID] | Ruiguo Wang[1] | John P. Giesy[2,3,4,5] | Su Zhang[1] | Shulin Wei[1] | Peilong Wang[1]

[1]Institute of Quality Standard and Testing Technology for Agro-Products, Chinese Academy of Agricultural Sciences, Beijing, China

[2]Department of Veterinary Biomedical Sciences and Toxicology Centre, University of Saskatchewan, Saskatoon, Saskatchewan, Canada

[3]Department of Zoology and Center for Integrative Toxicology, Michigan State University, East Lansing, Michigan, USA

[4]Department of Environmental Sciences, Baylor University, Waco, Texas, USA

[5]State Key Laboratory of Pollution Control and Resource Reuse, School of the Environment, Nanjing University, Nanjing, China

Correspondence
Peilong Wang, Institute of Quality Standard and Testing Technology for Agro-Products, Chinese Academy of Agricultural Sciences, No.12 Zhongguancun South Street, Haidian District, Beijing 100081, China.
Email: wangpeilong@caas.cn

Funding information
Science and Technology Innovation Program of the Chinese Academy of Agricultural Sciences; Fundamental Research Funds for Central Public Research Institutes, Grant/Award Number: Y2020PT38; National Natural Science Foundation of China, Grant/Award Number: 31602117; National Key Research and Development Program of China, Grant/Award Number: 2017YFC1600300

Abstract

Tris (1,3-dichloro-2-propyl) phosphate (TDCIPP) is one of the most commonly used organophosphorus flame retardants. Immuno-toxicity induced by TDCIPP is becoming of increasing concern. However, effects of TDCIPP on immune cells and mechanisms resulting in those effects are poorly understood. In this study, it was determined, for the first time, by use of isobaric tags for relative and absolute quantification (iTRAQ) based proteomic techniques expression of global proteins in RAW264.7 cells exposed to 10 μM TDCIPP. A total of 180 significantly differentially expressed proteins (DEPs) were identified. Of these, 127 were up-regulated and 53 were down-regulated. The DEPs associated with toxic effects of TDCIPP were then screened by use of Gene Ontology and the Kyoto Encyclopedia of Genes and Genomes for enrichment analysis. Results showed that these DEPs were involved in a number of pathways including apoptosis, DNA damage, cell cycle arrest, immune-toxicity, and signaling pathways, such as the Toll-like receptor, PPAR and p53 signaling pathways. The complex regulatory relationships between different DEPs, which might play an important role in cell death were also observed in the form of a protein–protein interaction network. Meanwhile, mitochondrial membrane potential (MMP) in RAW264.7 cells after TDCIPP treatment was also analyzed, the collapse of the MMP was speculated to play an important role in TDCIPP induced apoptosis. Moreover, some of the important regulator proteins discovered in this study, such as Chk1, Aurora A, would provide novel insight into the molecular mechanisms involved in toxic responses to TDCIPP.

KEYWORDS
apoptosis, iTRAQ, proteomics, RAW264.7 cells, toxicology, tris (1,3-dichloro-2-propyl) phosphate

1 | INTRODUCTION

Flame retardants (FR) are frequently added to a wide range of materials, including electronics, textiles and furniture. In recent years, brominated flame retardants, including polybrominated diphenyl ethers (PBDEs) have been phased out after being listed in the Stockholm convention on persistent organic pollutants (Dishaw et al., 2014; Wang, Chen, et al., 2020). Organophosphorus flame

retardants (OPFRs), as an alternative, have been increasingly used in various products (Castro-Jiménez et al., 2016), with global consumption reaching ∼680,000 t in 2015 (Cui et al., 2020). Tris (1,3-dichloro-2-propyl) phosphate (TDCIPP), as one of the most commonly used OPFRs, has been wildly applied in plastics, foams, electronics equipment, and furniture (Dishaw et al., 2014; Li et al., 2015). Annual production of TDCIPP in the United States, in 1998 and 2008 is reported to have been 4500 and 22,700 t, respectively (van der Veen & de Boer, 2012).

TDCIPP has been detected in a wide range of environmental media. TDCIPP was detected in seawater from three coastal cities at concentrations from 24.0 to 377.9 ng/L (Hu et al., 2014) and in water from the Songhua River at concentrations of 2.5–40 ng/L (Wang et al., 2011) in China. TDCIPP was also found in food of humans, such as cereals (<0.5–0.89 ng/g wm), vegetables (<0.05–1.06 ng/g wm), fruits (<0.15–0.57 ng/g wm), and meat (<0.2–0.52 ng/g wm) (Poma et al., 2017). Moreover, TDCIPP and its metabolite (bis(1,3-dichloro-2-propyl) phosphate; BDCIPP) were detected in human milk and urine of office workers, which indicated that humans are exposed to TDCIPP and could thus be at risk of adverse effects (Carignan et al., 2013; Sundkvist et al., 2010).

TDCIPP can cause neurotoxicity, developmental toxicity, endocrine disruption, hepatotoxicity (Farhat et al., 2014; Li et al., 2015; Liu et al., 2019; Slotkin et al., 2017). Immune cells were also targets of TDCIPP and other OPFRs. TDCIPP was reported to disrupt the inflammatory balance by inhibiting both proinflammatory and antiinflammatory cytokines in human THP-1-derived macrophages, and caused a functional loss of phagocytosis, implying the potential immunosuppression (Li et al., 2020). TDCIPP was cytotoxic to bone marrow-derived dendritic cells (BMDCs) with concentration ≥50 μM, and suppressed the expression of MHCII and the IL-6 production (Canbaz et al., 2017). Mechanisms of toxicity in different cells induced by TDCIPP, such as skin keratinocytes, neuronal cells and hepatocellular cells, were widely reported (Crump et al., 2012; Cui et al., 2020; Hao et al., 2019). TDCIPP decreased cell viability, induced cell cycle arrest, DNA damage and apoptosis. However, the mechanisms of toxic actions of TDCIPP in immune cells are still limited.

Isobaric tags for relative and absolute quantification (iTRAQ) is an effective method of analyzing differences in proteomes between normal and pathological states in cells or tissues (Wang, Yang, et al., 2020). Recently, iTRAQ was applied in toxicological research on environmental pollutants. Gender-specific responses in mussel *Mytilus galloprovincialis* to Tetrabromobisphenol A (TBBPA) was analyzed by iTRAQ-based proteomics. Most of the differentially expressed proteins (DEPs) were functionally mapped to reproduction and development, metabolism, signal transduction, gene expression, stress response and apoptosis (Ji et al., 2014). Proteomics and metabolomics were integrated to analyze the proteome and metabolome responses in rockfish *Sebastes schlegeli* treated with tris(1-chloro-2propyl) phosphage (TCIPP), which is one of the most frequently and abundantly detected OPFRs (Ji et al., 2020). DEPs were mainly associated with TCIPP induced neurotransmission, neurodevelopment, signal transduction, transport, metabolism, and detoxification.

Results of our previous studies indicated that TDCIPP could induce cytotoxicity in RAW264.7 macrophage cells, which resulted in DNA damage, cell cycle arrest, and apoptosis (Zhang, Wang, et al., 2019). To identify molecular events and pathways potentially involved in TDCIPP toxicities, proteomic analysis based on iTRAQ was therefore used to analyze global expressions of proteins in RAW264.7 cells exposed to TDCIPP. Changes and regulatory relationships of these DEPs can thus be used to determine the complex toxicological effects of TDCIPP on RAW264.7 cells, which will contribute to establish a better understanding of molecular mechanisms of TDCIPP toxicities on macrophages.

2 | MATERIALS AND METHODS

2.1 | Materials

TDCIPP (CAS no. 13674-87-8, 95.6% purity) was purchased from Sigma-Aldrich (St. Louis, Missouri, USA) and was dissolved in dimethyl sulfoxide (DMSO) as a stock solution. Mouse anti-Chk1, rabbit anti-c-Jun, rabbit anti-Atg7, rabbit anti-β-actin, horse anti-mouse IgG and goat anti-rabbit IgG were obtained from Cell Signaling Technology (Danvers, Colorado, USA), rabbit anti p53R2 + RRM2, rabbit anti-CKS2, mouse anti-Aurora A were purchased from Abcam (Cambridge, U.K.). Chemicals for sodium dodecyl sulfate polyacrylamide gel electrophoresis (SDS-PAGE) were obtained from Genscript (Nanjing, China).

2.2 | Cell culture and treatment

RAW264.7 cells were obtained from the Stem Cell Bank, Chinese Academy of Sciences, and were cultured in Dulbecco's modified Eagle's medium (DMEM) supplemented with 100-U/ml penicillin, 100-μg/ml streptomycin (Macgene, Beijing, China), and 10% fetal bovine serum (Gibco, Waltham, MA, USA) at 37°C in a humidified atmosphere containing 5% CO_2. Based on our previous results, TDCIPP could induce significant DNA damage, cell cycle arrest and apoptosis at a concentration of 10 μM (Zhang, Wang, et al., 2019). Therefore, in this study, the RAW264.7 cells were seeded in 10-mm dish at a cell density of 1×10^4. Cells were then treated with 10 μM of TDCIPP for 24 hr before further proteomics analysis. Control cells were incubated with 0.1% DMSO to match the final concentration achieved in culture medium in the experimental exposures (Figure 1A).

2.3 | Mitochondrial membrane potential analysis

Previously published results showed that exposure to various concentrations of TDCIPP (0, 0.1, 1, 10, 50, or 100 μM) affected viabilities of RAW264.7 cell and resulted in greater intracellular concentrations of reactive oxygen species (ROS) (Zhang, Wang et al., 2019). In this
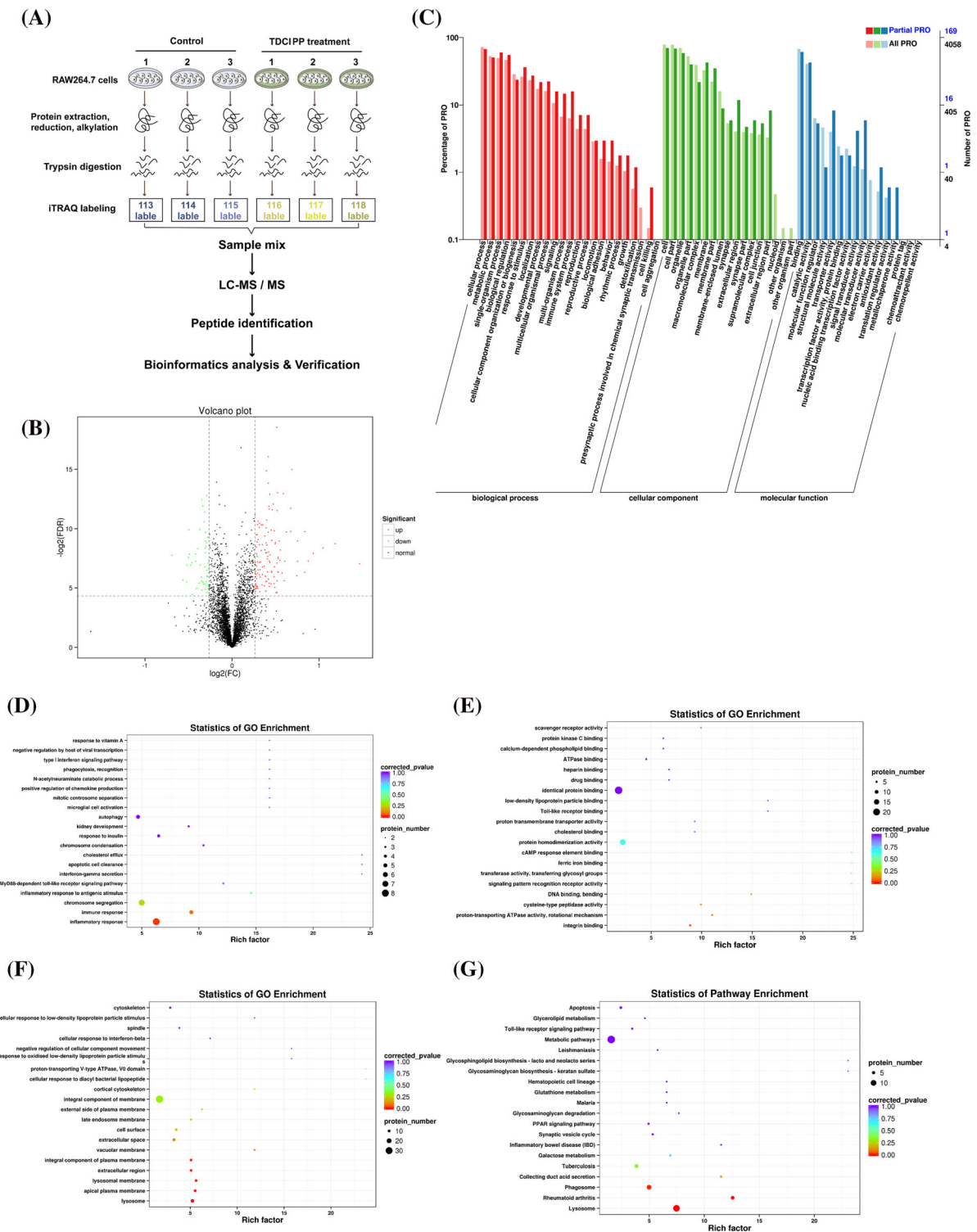
FIGURE 1 (A) Schematic of the experimental design and workflow for quantitative identification of the proteomes in RAW264.7 cells exposed to tris (1,3-dichloro-2-propyl) phosphate (TDCIPP). (B) Volcano plot of the protein ratio. Red dots denote up-regulated proteins and green dots denote down-regulated proteins. (C) Gene ontology (GO) annotation analysis of differentially expressed proteins (DEPs). All identified proteins were functionally annotated in the GO database according to biological process (red), cellular component (green), and molecular function (blue). (D–F) GO enrichment analysis of DEPs. The GO terms of 20 most significantly changed proteins identified from the comparison between TDCIPP and control group in biological process (D), cellular component (E), and molecular function (F). (G) Scatter plot showing the Kyoto encyclopedia of genes and genomes (KEGG) pathway enrichment levels of the DEPs between TDCIPP and control group

study, the mitochondrial membrane potential (MMP) assay was performed with a mitochondrial probe (JC-1). JC-1 was dissolved and stored according to the manufacturer's instruction. After treated with various concentrations of TDCIPP (0, 0.1, 1, 10, 50, or 100 μM) for 24 hr, cells were collected and the cell suspension was adjusted to a density of 1×10^6 cells/ml and incubated in complete medium for 20 min at 37°C in dark with 10 μg/ml JC-1. Then, the fluorescence intensity was determined using a FACSCalibur flow cytometer (BD Biosciences, San Jose, CA, USA). A minimum of 1×10^5 cells were collected for flow cytometry analysis.

2.4 | iTRAQ labeling and strong fractionation by cation exchange chromatography

Protein peptides from each group (0 and 10 μM TDCIPP) were labeled using the 8-plex iTRAQ reagents multiplex kit (ABI, Foster City, CA, USA) (isobaric tags 113, 114, and 115 for the control group and isobaric tags 116, 117, and 118 for the TDCIPP treated group). Protein samples (200 μg) were precipitated with 10 volumes of acetone overnight at −20°C. Protein pellets were dissolved in 60 μl of iTRAQ dissolution buffer (Applied Biosystems) after centrifugation for 10 min at 15300×g. The 8-plex iTRAQ reagents were reconstituted with 50 μL isopropyl alcohol, then added to the corresponding peptide samples and reacted at room temperature for 1 hr. A 100-μl aliquot of water was added to stop the labeling reaction. A 1-μl aliquot of sample was removed from each group to test labeling and extraction efficiency. Then, samples were subjected to a matrix assisted laser desorption ionization procedure after Ziptip desalting. Samples were pooled and vacuum-dried. Each pool of mixed peptides was lyophilized and dissolved in solution A (2% acetonitrile [ACN] and 20 mM ammonium formate, pH 10). Samples were then loaded onto a reverse-phase column (Luna C18, 4.6×150 mm; Phenomenex, Torrance, CA, USA) and eluted using a step linear elution program: 0%–10% buffer B (500 mM KCl, 10 mM KH_2PO_4 in 25% ACN, pH 2.7) for 10 min, 10%–20% buffer B for 25 min, 20%–45% buffer B for 5 min, and 50%–100% buffer B for 5 min at a flow rate of 0.8 ml/min. Samples were collected each min and centrifuged for 5–45 min. Fractions collected were combined into 6 pools and desalted on C18 Cartridges (Empore™ standard density SPE C18 Cartridges, bed I.D. 7 mm, 3 mL volume, Sigma, St. Louis, MO, USA).

2.5 | LC-electrospray ionization-MS/MS analysis

Reconstituted peptides were analyzed with the Q-Exactive mass spectrometer (Thermo Fisher Scientific, Waltham, MA, USA) coupled with a nano high-performance liquid chromatography (UltiMate 3,000 LC Dionex, Thermo Fisher Scientific) system. Collected peptides were loaded onto a C18-reversed phase column (3-μm C18 resin, 75 μm × 15 cm) and separated on an analytical column (5-μm C18 resin, 150 μm × 2 cm, Dr. Maisch GmbH, Ammerbuch, Germany) using mobile phase A (0.5% formic acid [FA]/H_2O) and B (0.5% FA/CAN) at a flow rate of 300 nl/min. Spectra were acquired in data-dependent mode. The 10 most intense ions selected for MS scanning (300–1800 m/z, 60,000 resolutions at m/z 400, accumulation of 1×10^6 ions for a maximum of 500 ms, 1 microscan). The isolation window was 1.3 m/z, and the MS/MS spectra were accumulated for 150 ms using an Orbitrap. MS/MS spectra were measured at resolution of 15,000 at m/z 400. Dynamic precursor exclusion was allowed for 120 s after each MS/MS spectrum was collected and was set to 17,500 at m/z 200. Normalized collision energy was 30 eV and the under fill ratio, which specifies the minimum percentage of the target value likely to be reached at the maximum fill time, was defined as 0.1%.

2.6 | Sequence database search and data analysis

Proteome Discoverer 2.1 (V2.1, Thermo Fisher Scientific) software was used for data analysis. Peptide identification was performed with the SEQUST search engine using mouse proteome databases containing reviewed Uniprot sequences downloaded from Uniprot. Decoys for the database search were generated with the revert function. Parameters were set as follows: Peptide mass tolerance = ±15 ppm, MS/MS tolerance = 0.02 Da, enzyme = trypsin, missed cleavage = 2, fixed modification: iTRAQ-8plex (K) and iTRAQ-8plex (N-term), Carbamidomethyl (C), variable modification: oxidation (M), database pattern = decoy. The false discovery rate (FDR) for peptides and proteins was set to 0.01.

2.7 | Proteomic data analysis and bioinformatics analyses

The UniProt database (https://www.uniprot.org/) was selected as the reference database for peptide and protein identification. DEPs were identified by the threshold of fold change value ≥1.2 and p values ≤0.05. The functional enrichment of Gene Ontology (GO) terms and the Kyoto Encyclopedia of Genes and Genomes (KEGG) pathways was performed for DEPs in the DAVID database (https://david.ncifcrf.gov/) and KEGG PATHWAY Database (http://www.genome.jp/kegg/). The STRING database (https://string-db.org) and Cytoscape software 3.8 (https://cytoscape.org) were used for protein–protein interaction (PPI) network analysis.

2.8 | Western blot analysis

Expressions of proteins including Chk1, c-Jun, CKS2, Aurora A, RRM2 and Atg7 were quantified by use of western blot. Briefly, cells were seeded in 10-mm dishes for exposure to TDCIPP for 24 hr, after which cells were harvested and lysed in the lysis buffer containing 1 mM phenylmethylsulfonyl fluoride (Macgene, Beijing, China). Samples were centrifuged at 16,900 g for 10 min at 4°C. Concentrations of protein were determined by use of the BCA Protein Assay Kit

(CST, Danvers, Colorado, USA). Each sample (20–30 μg) was loaded and electrophoresed on 10% SDS-PAGE. Proteins were transferred to PVDF membrane after electro-blotting at 4°C. Subsequently, membranes were blocked with 5% skim milk and incubated with specific antibodies (anti-β-actin, anti-Chk1, anti-c-Jun, anti-CKS2, anti-Aurora A, anti-p53R2 + RRM2 and anti-Atg7) at 1:1000 dilution at 4°C overnight. Subsequently, membranes were then incubated with the HRP-conjugated goat anti-rabbit IgG or goat anti-mouse IgG secondary antibodies (1:4000) at room temperature for 1 hr. The protein signals were visualized by enhanced chemi-luminescence (ECL) system. Relative expression of each protein was calculated by normalization to β-actin, and the resulting ratios in the control group were normalized to 1.

2.9 | RNA extraction and qRT-PCR

Total RNA was extracted using the RNAprep Pure Cell/Bacteria Kit (Tiangen, Beijing, China) following the manufacturer's instruction. Reverse transcription of RNA and PCR amplification was performed using the One Step TB Green PrimeScript RT-PCR Kit II (Takara Bio, Otsu, Shiga, Japan). The PCR mixture consisted of 10 μl of 2 × One Step TB Green RT-PCR buffer, 0.8 μl of PrimeScript 1 Step Enzyme mix 2, 0.8 μl of forward primer, 0.8 μl of reverse primer, 0.4 μl of ROX Reference Dye II, 2 μl of total RNA, and 5.2 μl of RNase Free dH$_2$O in a total volume of 20 μL. PCR primers were listed in Table S1. The qRT-PCR was carried out with an Applied Biosystems QuantStudio 5 Real-Time PCR System (Applied Biosystems, Foster City, CA, USA). Target gene expression levels were normalized to *GAPDH* expression values and calculated using the $2^{-\Delta\Delta CT}$ method (Livak & Schmittgen, 2001).

2.10 | Statistical analyses

Experiments were performed at least three times. Values are reported as mean±standard deviation (SD). All data were processed with SPSS 22.0 for windows (SPSS Inc., Chicago, IL, USA). A Shapiro–Wilks normality test indicated that the results were normally distributed. The assumption of homogeneity of variance was assessed using Levene' test. The statistical significance of differences was determined by use of one-way analysis of variance (ANOVA). A value of $p < 0.05$ was considered statistically significant.

3 | RESULTS

3.1 | Mitochondrial membrane potential analysis

Mitochondrial membrane potential is one of the important indicators for maintaining normal mitochondrial configuration and function. Decreased MMP is considered to be an important factor leading to apoptosis. Influence of TDCIPP on MMP in RAW264.7 cells was then

evaluated. In this study, MMP in RAW264.7 cells treated with TDCIPP (1–100 μM) were significantly decreased when compared to the control group (Figure 2).

3.2 | Protein identification and quantification

A total of 4330 proteins were successfully identified by iTRAQ quantitative analysis, with 180 significant DEPs between the two groups (0 and 10 μM TDCIPP) according to the level of differential expression (filtered according to fold changes ≥1.2, and p values ≤0.05). Of these, 127 were up-regulated and 53 were down-regulated (Figure 1B and Table S2).

3.3 | GO analysis of differentially expressed proteins

To functionally classify the differentially expressed proteins between control and TDCIPP treated groups, GO analysis was performed with proteins categorized according to biological processes (BP), cellular components (CC), and molecular functions (MF) (Figure 1C). In the BP category, cellular process, metabolic process, single-organism process and biological regulation were the main subcategories. Cell, cell part, organelle and membrane are the four main subcategories in CC category. In the MF category, binding and catalytic activity are the two main subcategories.

Enriched analyses of GO terms were also performed on differentially expressed proteins revealed between control and TDCIPP treated groups. GO terms were enriched according to BP, CC and MF independently. A scatter plot demonstrates levels of enrichment of the DEPs in BP, CC and MF (Figure 1D–F). The GO terms "autophagy," "chromosome segregation," "immune response," "inflammatory response," and "MyD88-dependent toll-like receptor signaling pathway" were significantly enriched in BP. Meanwhile, "integral component of membrane," "lysosome," and "lysosome
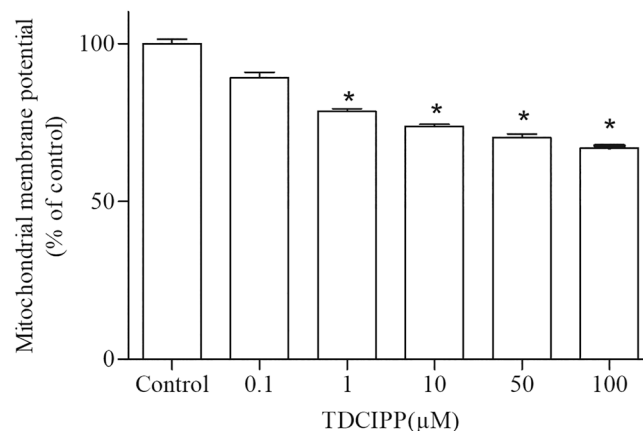

FIGURE 2 TDCIPP induced decreased mitochondrial membrane potential (MMP) in RAW264.7 cells. The data were shown as the mean±SD, * $p < 0.05$, compared with solvent control group

membrane" were enriched in CC. In MF, the enriched GO terms were mainly involved in "identical protein binding" and "protein homo-dimerization activity." It was speculated that DEPs in these GO terms are closely related to mechanisms responsible for toxicity of TDCIPP, especially for immune function of macrophages.

3.4 | KEGG pathway analysis of differentially expressed proteins

Multiple pathways were significantly enriched as determined by KEGG analysis. These included apoptosis, Toll-like receptor signaling pathway, PPAR signaling pathway (Figure 1G and Table S3). For instance, proteins were enriched for apoptosis (Cathepsin L, Cathepsin D, Cathepsin Z, Jun), PPAR signaling pathway (Cd36, Lpl, Fabp5), p53 signaling pathway (Chk1, RRM2), Toll-like receptor signaling pathway (Tlr2, Jun, Tlr7). These pathways had regulatory effects on cell cycle arrest, apoptosis, autophagy and immune function. Therefore, these signaling pathways could be targets of subsequent research on the toxic mechanism of TDCIPP toward macrophages. Meanwhile, enrichment of proteins in KEGG pathway was well correlated with the enriched proteins in GO enrichment.

3.5 | Protein–protein interaction network

TDCIPP was observed to cause cell cycle arrest and apoptosis during the study, results of which are presented here. Thus, protein–protein

interactions (PPI) between various DEPs might play important roles in cell death progress were constructed by use of the STRING database and analyzed by use of Cytoscape 3.8 (Figure 3). Differentially expressed proteins were closely associated with apoptosis, DNA integrity checkpoint, oxidative stress, redox, autophagy and Toll-like receptor signaling pathways. Proteins including Aurora A (Aurka), Chk1, CKS2, Top2a, Incenp, Trex1 are associated with cell cycle and mitosis related GO terms, such as chromosome condensation, centrosome cycle, DNA integrity checkpoint. CD36, Jun, Atg7, Prosaposin (Psap) are associated with ROS related GO terms. Cathepsin B, Cathepsin D, CathepsinL, CathepsinZ, Tlr2, Parp4 are associated with apoptosis. Overall, the protein–protein interaction network exhibited the complex regulatory relationships occurring between exposure to TDCIPP, DEPs, and signaling pathways.

3.6 | Confirmation of selected DEPs compared with iTRAQ database

Six proteins selected to validate by use of western blotting included: Chk1, c-Jun, CKS2, Aurora A, RRM2, and Atg7. These were selected because they were identified as DEPs with marked differences in expression between control group and TDCIPP group based on iTRAQ-based quantitative analysis (Figure 4). Chk1, RRM2, Aurora A, and CKS2 had lesser expression compared to those from control groups with a significant difference ($p < 0.05$). In contrast, significantly ($p < 0.05$) greater expressions of proteins, including c-Jun and Atg7 were observed in cells exposed to TDCIPP, compared with those from

FIGURE 3 Interaction network showing the protein–protein interactions occurring between the different differentially expressed proteins (DEPs) (generated using the CluePedia plugin of Cytoscape). Red and blue circle show up-regulated and down-regulated proteins, respectively. Orange solid circle refer to different gene ontology (GO) terms

FIGURE 4 Validation of altered protein expression in total cell lysates. Expression of Atg7, Aurora a, Chk1, c-Jun, CKS2, and RRM2 in cells treated with 10-μM TDCIPP, determined using Western blotting. Transcription of protein relative to the control group was normalized to β-actin. Values were expressed as the mean±SD. Statistical significance (* $p < 0.05$, compared with solvent control group) of protein expression levels was analyzed by independent-samples t-tests using SPSS22.0
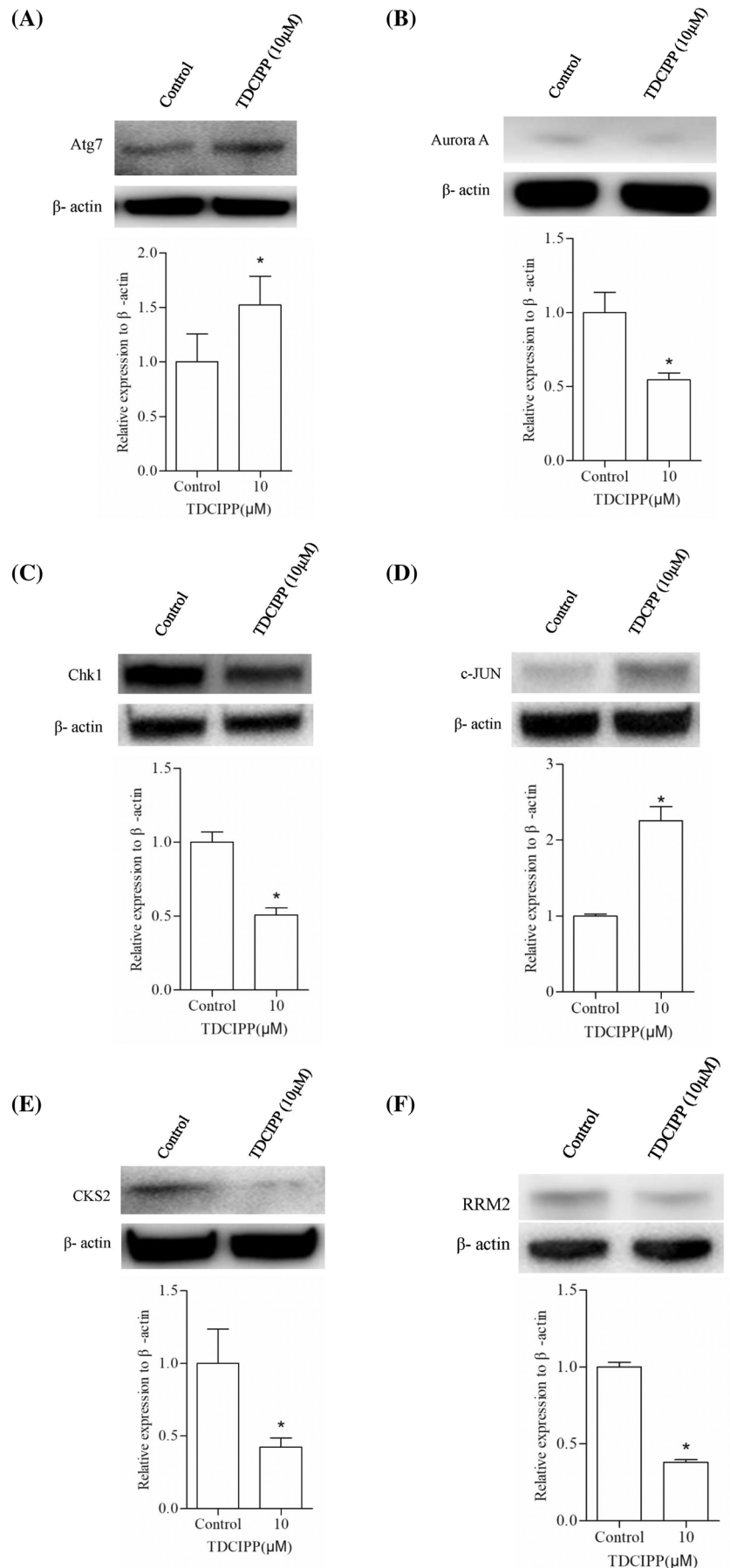
the controls. These results are consistent with the findings in iTRAQ-based quantitative analysis.

3.7 | Correlation between gene expressions and protein abundances

To further analyze the correlation between protein and gene expressions, six genes related to altered proteins, including Atg7, Aurora A, Chk1, c-Jun, CKS2, and RRM2, were quantified using qRT-PCR. Results indicated that mRNA expression levels of five selected genes (*Atg*7, *Aurora a*, *Chk*1, *c-Jun*, and *CKS*2) had consistent alteration tendency with corresponding proteins in TDCIPP treated group. Slightly but not statistically significant elevated expression level of *RRM*2 was presented, while the protein level was down-regulated (Figure S1).

4 | DISCUSSION

TDCIPP exhibited various toxicities in various types of cells (Cui et al., 2020; Killilea et al., 2017; Li et al., 2017), including immune cells (Canbaz et al., 2017). Results of previous studies of toxicological effects of TDCIPP in mouse macrophage RAW264.7 cells in vitro, demonstrated increased intracellular concentrations of ROS, cell cycle arrest and apoptosis (Zhang, Wang, et al., 2019), but mechanism of these effects of TDCIPP on macrophage cells still needed further elucidation. Therefore, further research on effects of TDCIPP was conducted by use of iTRAQ analysis. DEPs observed in RAW264.7 cells exposed to TDCIPP were investigated by use of iTRAQ technology, intended to elucidate the overall protein changes which are involved in toxic effects of TDCIPP and cellular adaptive responses.

Since mitochondria are considered to not only be a major source of ROS, but also the target of cellular ROS (Erikstein et al., 2010; Jiang et al., 2020), changes in MMP of RAW264.7 cells was examined by use of JC-1 staining. TDCIPP caused the collapse of MMP. It has been shown previously that mitochondrial disorders can result in lesser MMP and decrease activity of the respiratory chain with a simultaneously greater production of ROS. Decreased MMP was an important factor, which could cause apoptosis and was considered to be the first step of the apoptosis cascade during programmed cell death (Zhang, Zhang, et al., 2019). Therefore, combined with previous observations that TDCIPP induced increased concentrations of intracellular ROS and Caspase-3, it was hypothesized that the mitochondrial pathway might have participated in apoptosis induced by exposure to TDCIPP.

DEPs from exposure to TDCIPP, when compared to controls by GO classification, suggested that proteins might play diverse regulatory roles in cytotoxicity caused by exposure of RAW264.7 cells to TDCIPP. In MF and BP classification, the dominant enrichment of binding protein was closely related to responses to stimuli. In terms of CC classification, membrane was enriched. Similar results have been previously reported (Yang et al., 2019). Macrophages play an important role in immunity (Wynn et al., 2013) and express various receptors, such as Toll-like receptors, that mediate their diverse functions, including antigen presenting and phagocytosis. These receptors are located on the surface as well as in vacuolar compartments and the cytosol, thereby mediating recognition of extracellular and intracellular pathogens (Gordon, 2007). Therefore, it was speculated that there was a correlation between the toxicological effects of TDCIPP, especially the immune toxicity of macrophages, and the aforementioned GO terms.

GO enrichment analysis was conducted to investigate classes of proteins associated with toxic effects of TDCIPP. GO term results showed that DEPs mainly regulated autophagy, cell cycle in GO scatter plot. Proteomic changes were the same as the phenomenon exhibited in RAW264.7 cells exposed to 10-μM TDCIPP, which induced cell cycle arrest (Zhang, Zhang, et al., 2019). Meanwhile, since the GO terms of immune response, inflammatory response, integral component of membrane, lysosome, and lysosome membrane were enriched, the results indicated that DEPs might have participated in the immuno-toxicity caused exposure of RAW264.7 to TDCIPP. Autophagy is the major intracellular degradation system by which cytoplasmic materials are delivered to and degraded in the lysosome (Mizushima & Komatsu, 2011). Perfluorooctane sulfonate (PFOS) can cause dysfunction of mitochondria via blocking autophagy-lysosome degradation, which resulted in cardiomyocyte toxicity in embryonic stem cells (Liu et al., 2020). Thus, GO enrichment results we obtained provided more information for understanding the relationship between lysosome and autophagy in RAW264.7 cells exposed to TDCIPP.

Subsequent KEGG pathway enrichment indicated that toxic effects caused by exposure of RAW264.7 cells to TDCIPP were closely related to several pathways (Figure 1G), which were associated with cell cycle arrest and apoptosis, which had been observed previously. Meanwhile, some of these pathways might involve dysregulation of immune function caused by TDCIPP in macrophages. Toll-like receptors (TLRs), such as TLR2, TLR4, played an essential role in detection of invading pathogens and induction of host antimicrobial defenses. Also, TLR signaling has different effects on apoptosis (Sabroe et al., 2005). For instance, TLR4 can activate a Jun N-terminal kinase (JNK)/caspase-dependent pathway of apoptosis in endothelial cells (Hull et al., 2002), whereas TLR2 signals for apoptosis through myeloid differentiation factor (MyD88) via a pathway involved Fas-associated death domain protein and caspase 8 (Aliprantis et al., 2000). Interestingly, some studies have demonstrated functions of TLR in regulation of cell cycle (Arcangeletti et al., 2013). The p53 signaling pathway played an important role in cellular responses to diverse stress stimuli, such as chemicals that damage DNA or cause hypoxia or activation of oncogenes. The p53 is at the center of an intricate regulatory protein network exhibiting diverse and systemic functions, including cell cycle arrest, senescence and apoptosis (Amaral et al., 2009; Engeland, 2018). Therefore, it was hypothesized that the p53 signaling pathway might participate in regulation of cell cycle arrest and apoptosis caused by exposure of RAW264.7 cells to

TDCIPP. Hypothetical mechanisms related to the proteomic response of RAW264.7 cells to TDCIPP are given (Figure 5).

The protein–protein interaction network provides insights that significantly complement data obtained from quantitative proteomics. PPI results indicated that some proteins, such as Chk1, Cathepsin D, Atg7, CD36, Jun, Psap, and Aurora A (Aurka), were connected with more different pathways which were associated with cell death progress, including apoptosis, cell cycle, autophagy and ROS regulation. The interaction network showed clearly how a given protein regulated multiple pathways, illustrated the complex regulatory relationship between the DEPs and signaling pathways. The pathways and proteins highlighted provide information for elucidation of mechanisms responsible for toxic effects of TDCIPP, and are thus helpful in focusing subsequent studies of toxic effects of TDCIPP, such as immune-toxicity.

Checkpoint kinases 1 (Chk1) are core protein kinases in genome surveillance pathways, which preserve genome integrity (Reinhardt & Yaffe, 2009). Chk1 was activated by damage to DNA, which then transduced the checkpoint signal and facilitated cell cycle arrest and repair of damage to DNA (Zhang & Hunter, 2014). It was the key downstream regulator of the cell cycle checkpoint proteins ataxia-telangiectasia-mutated-and-Rad3-related kinase (ATR) and is phosphorylated by ATR on Ser-317 and Ser-345 (Liu et al., 2000; Qiu et al., 2018). Activated Chk1 triggered the intra-S and G2/M-phase checkpoints (Dai & Grant, 2010). In this study, Chk1 was down-regulated in RAW264.7 cells exposed to TDCIPP (Figure 4C). It has

been previously reported that TDCIPP could induce G2/M phase arrest (Zhang, Zhang, et al., 2019), but details of the mechanisms remain unelucidated.

Meanwhile, our data indicated that the cyclin-dependent kinase subunit 2 (CKS2) was significantly down-regulated in cells exposed to TDCIPP (Figure 4E). CKS proteins are an evolutionarily conserved subunit of the cyclin-dependent protein kinases (CDKs) that regulate mitosis in all eukaryotes (Frontini et al., 2012; Pines, 1996). It has been reported that Cks2 down-regulation inhibited cholangiocarcinoma cell proliferation. Furthermore, Cks2 knockdown induced cholangiocarcinoma cell cycle arrest in G2/M phase through down-regulation of Cyclin A and Cyclin B1 (Shen et al., 2013). Down-regulation of Cyclin B1 and G2/M phase arrest were also observed in our previous research (Zhang, Wang, et al., 2019). Additionally, decline of CKS2 expression was found concordantly with the increased apoptosis in HepG2 cells (Lin et al., 2016). So we speculated that CKS2 and Chk1 might involve in the G2/M phase arrest and apoptosis of RAW264.7 treated with TDCIPP.

Ribonucleotide reductase M2 (RRM2) is one of the small subunits in the activated form of mammalian ribonucleotide reductase (RR), which provides dNTPs during S/G2 phases for DNA replication in a cell-cycle-regulated manner in dividing cells (Gong et al., 2016). It has also been reported that RRM2 was activated during repair of DNA via the ATR-Chk1-E2F3 signaling pathway in response to exposure to carcinogens. Similar results have been reported by other groups (Anacker et al., 2016; Koppenhafer et al., 2020; Zhang et al., 2009).

FIGURE 5 Schematic of hypothetical mechanism indicated by altered proteins in RAW264.7 cells exposed to TDCIPP. TDCIPP exposure could induce the generation of reactive oxygen species (ROS) and damage DNA in RAW264.7 cells. ATR/Chk1/DCD25c pathway regulate cell cycle arrest induced by TDCIPP. The p53 and JNK pathway were involved in cell cycle arrest and apoptosis caused by TDCIPP. Up-regulated CathepsinB, D, L, Z, Atg7, and LAMP1/2, indicated that autophagy might play important role in TDCIPP induced cell death. In this model, the letters in bold demonstrated the important differentially expressed proteins related to the toxicity of TDCIPP. And the letters in orange bold represents the validate proteins by western blotting
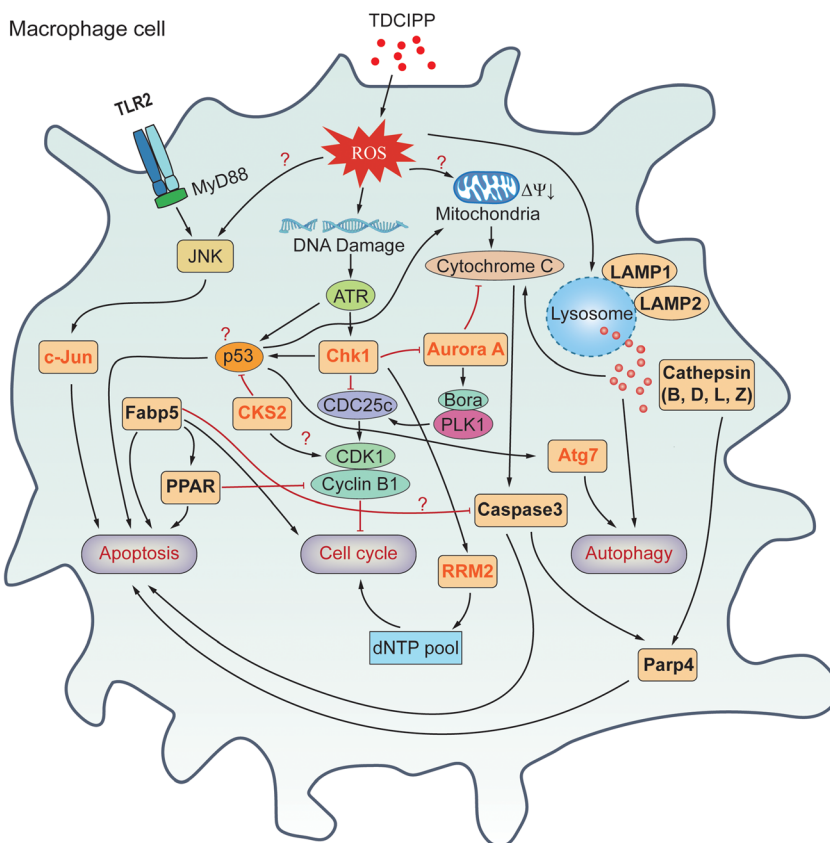
These results suggested that RRM2 might be associated with Chk1, which plays an important role in cell cycle arrest and apoptosis in cells exposed to TDCIPP (Gong et al., 2016).

The c-Jun is the founding member and the most potent transcriptional activator of the AP-1 family, and is involved in numerous cell activities, such as cell cycle, apoptosis, proliferation, survival, tumorigenesis (Meng & Xia, 2011). It was reported that c-Jun could activate cyclin D1 promoter, which finally regulated cell cycle progression (Bakiri et al., 2000). Overexpression of c-Jun repressed p53 and p21 expression and accelerated cell proliferation (Schreiber et al., 1999). Activation of c-Jun protein is regulated by several different mechanisms and signaling pathways, including the c-Jun N-terminal kinase (JNK) pathway (Fuchs et al., 1996). The JNK/c-Jun pathway was reported as a critical cascade in the process of heroin-induced neuronal apoptosis (Pu et al., 2015). These results provided potential connections of c-Jun, p53 and JNK in TDCIPP induced cell cycle arrest and apoptosis in RAW264.7 cells.

As one of the core protein in autophagic machinery, autophagy related 7 (Atg7) plays crucial roles in the two ubiquitin-like conjugation systems of microtubule-associated protein light chain 3 (LC3) and ATG12 respectively (Xiong, 2015). T-2 toxin could induce autophagy in chicken hepatocytes, the expression of Atg7 and other autophagy-related proteins were increased (Yin et al., 2020). Also, Atg7 could coordinates tumor suppressor p53-mediated cell division cycle and cell apoptosis via physical interaction with p53 (Lee et al., 2012). Atg7 was found up-regulated in TDCIPP treated RAW264.7 cells, whether TDCIPP could cause autophagy remain to be elucidated. Meanwhile, further exploration was needed to explore the potential role of p53 and Atg7 in TDCIPP induced cell cycle arrest.

Aurora Kinases are highly conserved serine/threonine kinases that regulated multiple events during cell cycle progression and essential for mitotic and meiotic bipolar spindle assembly and function (Damodaran et al., 2017; Goldenson & Crispino, 2015). Aurora A regulated the progression of mitosis by phosphorylation of multiple substrates and promoted mitotic entry by controlling activation of Cyclin B/Cdk-1 (Hirota et al., 2003). Aurora A promoted the localization of ATR to centromeres in mitosis (Kabeche et al., 2018). Another research reported that Aurora A could interact with Cyclin B1 and enhanced its stability (Qin et al., 2009). Aurora A activity might also be regulated by Chk1 kinase (Cazales et al., 2005). These results provided new insight into the mechanism of how deregulated Aurora A contributes to genomic instability and carcinogenesis. In our research, Aurora A was down-regulated in TDCIPP treated group (Figure 4B), and we suspected that it might be coordinated with Chk1 and CKS2 in G2/M phase arrest in RAW264.6 cells exposed to TDCIPP as observed in previous investigations.

The expression of six selected genes corresponding to Atg7, Aurora A, Chk1, c-Jun, CKS2 and RRM2 were quantified to evaluate the correlation between mRNA and protein expression levels. Five genes, with the exception of *RRM2*, exhibited consistent alteration tendency with corresponding proteins. The disparity between mRNA and protein expression was related to the posttranscriptional and posttranslational modifications, which were reported elsewhere (Ji et al., 2014; Wang et al., 2010).

5 | CONCLUSIONS

Here, for the first time, proteins that were significantly differentially expressed in RAW264.7 cells exposed and unexposed to TDCIPP were identified by use of iTRAQ-based proteomics. The results reported here indicated that complex networks of proteins and signaling pathways associated with certain DEPs, which were highly significant to a wide range of TDCIPP toxicological pathways. These included apoptosis, DNA damage, cell cycle arrest, immune-toxicity, and signaling pathways such as Toll-like receptor, PPAR and p53 signaling pathways (Figure 5). Combined with previously reported results, including the collapse of MMP after exposure to TDCIPP it can be postulated that the mitochondrial pathway might play important role in the apoptosis induced by TDCIPP. Furthermore, some of the important regulator proteins discovered in this study, such as Chk1, Aurora A, would provide novel insight into the molecular mechanisms involved in TDCIPP induced toxicity.

CONFLICT OF INTEREST

The corresponding author confirmed that the authors have no conflicts of interest with regard to the funding of this research.

DATA AVAILABILITY STATEMENT

The data that support the findings of this study are available from the corresponding author upon reasonable request.

ORCID

Wei Zhang https://orcid.org/0000-0002-2711-8020

REFERENCES

Aliprantis, A. O., Yang, R. B., Weiss, D. S., Godowski, P., & Zychlinsky, A. (2000). The apoptotic signaling pathway activated by toll-like receptor-2. *The EMBO Journal*, *19*, 3325–3336. https://doi.org/10.1093/emboj/19.13.3325

Amaral, J. D., Castro, R. E., Steer, C. J., & Rodrigues, C. M. P. (2009). p53 and the regulation of hepatocyte apoptosis: Implications for disease

pathogenesis. *Trends in Molecluar Medicine*, 15, 531–541. https://doi.org/10.1016/j.molmed.2009.09.005

Anacker, D. C., Aloor, H. L., Shepard, C. N., Lenzi, G. M., Johnson, B. A., Kim, B., & Moody, C. A. (2016). HPV31 utilizes the ATR-Chk1 pathway to maintain elevated RRM2 levels and a replication-competent environment in differentiating keratinocytes. *Virology*, 499, 383–396. https://doi.org/10.1016/j.virol.2016.09.028

Arcangeletti, M. C., Germini, D., Rodighiero, I., Mirandola, P., De Conto, F., Medici, M. C., Gatti, R., Chezzi, C., & Calderaro, A. (2013). Toll-like receptor 4 is involved in the cell cycle modulation and required for effective human cytomegalovirus infection in THP-1 macrophages. *Virology*, 440, 19–30. https://doi.org/10.1016/j.virol.2013.01.021

Bakiri, L., Lallemand, D., Bossy-Wetzel, E., & Yaniv, M. (2000). Cell cycle-dependent variations in c-Jun and JunB phosphorylation: A role in the control of cyclin D1 expression. *The EMBO Journal*, 19, 2056–2068. https://doi.org/10.1093/emboj/19.9.2056

Canbaz, D., Logiantara, A., van Ree, R., & van Rijt, L. S. (2017). Immunotoxicity of organophosphate flame retardants TPHP and TDCIPP on murine dendritic cells in vitro. *Chemosphere*, 177, 56–64. https://doi.org/10.1016/j.chemosphere.2017.02.149

Carignan, C. C., McClean, M. D., Cooper, E. M., Watkins, D. J., Fraser, A. J., Heiger-Bernays, W., Stapleton, H. M., & Webster, T. F. (2013). Predictors of tris(1,3-dichloro-2-propyl) phosphate metabolite in the urine of office workers. *Environment International*, 55, 56–61. https://doi.org/10.1016/j.envint.2013.02.004

Castro-Jiménez, J., González-Gaya, B., Pizarro, M., Casal, P., Pizarro-Álvarez, C., & Dachs, J. (2016). Organophosphate ester flame retardants and plasticizers in the global oceanic atmosphere. *Environmental Science & Technology*, 50, 12831–12839. https://doi.org/10.1021/acs.est.6b04344

Cazales, M., Schmitt, E., Montembault, E., Dozier, C., Prigent, C., & Ducommun, B. (2005). CDC25B phosphorylation by Aurora a occurs at the G2/M transition and is inhibited by DNA damage. *Cell Cycle*, 4, 1233–1238. https://doi.org/10.4161/cc.4.9.1964

Crump, D., Chiu, S., & Kennedy, S. W. (2012). Effects of tris(1,3-dichloro-2-propyl) phosphate and tris(1-chloropropyl) phosphate on cytotoxicity and mRNA expression in primary cultures of avian hepatocytes and neuronal cells. *Toxicological Sciences*, 126, 140–148. https://doi.org/10.1093/toxsci/kfs015

Cui, D., Bi, J., Zhang, Z. N., Li, M. Y., Qin, Y. S., Xiang, P., & Ma, L. Q. (2020). Organophosphorus flame retardant TDCPP-induced cytotoxicity and associated mechanisms in normal human skin keratinocytes. *Science of the Total Environmen*, 726, 138526. https://doi.org/10.1016/j.scitotenv.2020.138526

Dai, Y., & Grant, S. (2010). New insights into checkpoint kinase 1 in the DNA damage response signaling network. *Clinical Cancer Research*, 16, 376–383. https://doi.org/10.1158/1078-0432.CCR-09-1029

Damodaran, A. P., Vaufrey, L., Gavard, O., & Prigent, C. (2017). Aurora a kinase is a priority pharmaceutical target for the treatment of cancers. *Trends in Pharmacological Sciences*, 38, 687–700. https://doi.org/10.1016/j.tips.2017.05.003

Dishaw, L. V., Macaulay, L. J., Roberts, S. C., & Stapleton, H. M. (2014). Exposures, mechanisms, and impacts of endocrine-active flame retardants. *Current Opinion in Pharmacology*, 19, 125–133. https://doi.org/10.1016/j.coph.2014.09.018

Engeland, K. (2018). Cell cycle arrest through indirect transcriptional repression by p53: I have a DREAM. *Cell Death and Differentiation*, 25, 114–132. https://doi.org/10.1038/cdd.2017.172

Erikstein, B. S., Hagland, H. R., Nikolaisen, J., Kulawiec, M., Singh, K. K., Gjertsen, B. T., & Tronstad, K. J. (2010). Cellular stress induced by resazurin leads to autophagy and cell death via production of reactive oxygen species and mitochondrial impairment. *Journal of Cellular Biochemistry*, 111, 574–584. https://doi.org/10.1002/jcb.22741

Farhat, A., Buick, J. K., Williams, A., Yauk, C. L., O'Brien, J. M., Crump, D., Williams, K. L., Chiu, S., & Kennedy, S. W. (2014). Tris(1,3-dichloro-2-propyl) phosphate perturbs the expression of genes involved in immune response and lipid and steroid metabolism in chicken embryos. *Toxicology and Applied Pharmacology*, 275, 104–112. https://doi.org/10.1016/j.taap.2013.12.020

Frontini, M., Kukalev, A., Leo, E., Ng, Y. M., Cervantes, M., Cheng, C. W., Holic, R., Dormann, D., Tse, E., Pommier, Y., & Yu, V. (2012). The CDK subunit CKS2 counteracts CKS1 to control cyclin a/CDK2 activity in maintaining replicative fidelity and neurodevelopment. *Developmental Cell*, 23, 356–370. https://doi.org/10.1016/j.devcel.2012.06.018

Fuchs, S. Y., Dolan, L., Davis, R. J., & Ronai, Z. (1996). Phosphorylation-dependent targeting of c-Jun ubiquitination by Jun N-kinase. *Oncogene*, 13, 1531–1535.

Goldenson, B., & Crispino, J. D. (2015). The aurora kinases in cell cycle and leukemia. *Oncogene*, 34, 537–545. https://doi.org/10.1038/onc.2014.14

Gong, C., Liu, H., Song, R., Zhong, T., Lou, M., Wang, T., Qi, H., Shen, J., Zhu, L., & Shao, J. (2016). ATR-CHK1-E2F3 signaling transactivates human ribonucleotide reductase small subunit M2 for DNA repair induced by the chemical carcinogen MNNG. *Biochimica et Biophysica Acta (BBA) - Gene Regulatory Mechanisms*, 1859, 612–626. https://doi.org/10.1016/j.bbagrm.2016.02.012

Gordon, S. (2007). The macrophage: Past, present and future. *European Journal of Immunology*, 37, S9–S17. https://doi.org/10.1002/eji.200737638

Hao, Z., Zhang, Z., Lu, D., Ding, B., Shu, L., Zhang, Q., & Wang, C. (2019). Organophosphorus flame retardants impair intracellular lipid metabolic function in human hepatocellular cells. *Chemical Research in Toxicology*, 32, 1250–1258. https://doi.org/10.1021/acs.chemrestox.9b00058

Hirota, T., Kunitoku, N., Sasayama, T., Marumoto, T., Zhang, D., Nitta, M., Hatakeyama, K., & Saya, H. (2003). Aurora-A and an interacting activator, the LIM protein Ajuba, are required for mitotic commitment in human cells. *Cell*, 114, 585–598. https://doi.org/10.1016/s0092-8674(03)00642-1

Hu, M., Li, J., Zhang, B., Cui, Q., Wei, S., & Yu, H. (2014). Regional distribution of halogenated organophosphate flame retardants in seawater samples from three coastal cities in China. *Marine Pollution Bulletin*, 86, 569–574. https://doi.org/10.1016/j.marpolbul.2014.06.009

Hull, C., McLean, G., Wong, F., Duriez, P. J., & Karsan, A. (2002). Lipopolysaccharide signals an endothelial apoptosis pathway through TNF receptor-associated factor 6-mediated activation of c-Jun NH$_2$-terminal kinase. *The Journal of Immunology*, 169, 2611–2618. https://doi.org/10.4049/jimmunol.169.5.2611

Ji, C., Lu, Z., Xu, L., Li, F., Cong, M., Shan, X., & Wu, H. (2020). Global responses to tris(1-chloro-2-propyl)phosphate (TCPP) in rockfish *Sebastes schlegeli* using integrated proteomic and metabolomic approach. *Science of the Total Environment*, 724, 138307. https://doi.org/10.1016/j.scitotenv.2020.138307

Ji, C., Wu, H., Wei, L., & Zhao, J. (2014). iTRAQ-based quantitative proteomic analyses on the gender-specific responses in mussel *Mytilus galloprovincialis* to tetrabromobisphenol a. *Aquatic Toxicology*, 157, 30–40. https://doi.org/10.1016/j.aquatox.2014.09.008

Jiang, N., Wen, H., Zhou, M., Lei, T., Shen, J., Zhang, D., Wang, R., Wu, H., Jiang, S., & Li, W. (2020). Low-dose combined exposure of carboxylated black carbon and heavy metal lead induced potentiation of oxidative stress, DNA damage, inflammation, and apoptosis in BEAS-2B cells. *Ecotoxicology and Environmental Safety*, 206, 111388. https://doi.org/10.1016/j.ecoenv.2020.111388

Kabeche, L., Nguyen, H. D., Buisson, R., & Zou, L. (2018). A mitosis-specific and R loop–driven ATR pathway promotes faithful chromosome segregation. *Science*, 359, 108–114. https://doi.org/10.1126/science.aan6490

Killilea, D. W., Chow, D., Xiao, S. Q., Li, C., & Stoller, M. L. (2017). Flame retardant tris(1,3-dichloro-2-propyl)phosphate (TDCPP) toxicity is attenuated by *N*-acetylcysteine in human kidney cells. *Toxicology Reports*, 4, 260–264. https://doi.org/10.1016/j.toxrep.2017.05.003

Koppenhafer, S. L., Goss, K. L., Terry, W. W., & Gordon, D. J. (2020). Inhibition of the ATR-CHK1 pathway in Ewing sarcoma cells causes DNA damage and apoptosis via the CDK2-mediated degradation of RRM2. *Molecular Cancer Research*, *18*, 91–104. https://doi.org/10.1158/1541-7786.MCR-19-0585

Lee, I. H., Kawai, Y., Fergusson, M. M., Rovira, I. I., Bishop, A. J. R., Motoyama, N., Cao, L., & Finkel, T. (2012). Atg7 modulates p53 activity to regulate cell cycle and survival during metabolic stress. *Science*, *336*, 225–228. https://doi.org/10.1126/science.1218395

Li, C., Li, L., Lin, B., Fang, Y., Yang, H., Liu, H., & Xi, Z. (2017). Tris (1,3-dichloro-2-propyl) phosphate induces toxicity by stimulating CaMK2 in PC12 cells. *Environmental Toxicology*, *32*, 1784–1791. https://doi.org/10.1002/tox.22401

Li, J., Giesy, J. P., Yu, L., Li, G., & Liu, C. (2015). Effects of tris(1,3-dichloro-2-propyl) phosphate (TDCPP) in *Tetrahymena Thermophila*: Targeting the ribosome. *Scientific Reports*, *5*, 10562. https://doi.org/10.1038/srep10562

Li, X., Li, N., Rao, K., Huang, Q., & Ma, M. (2020). In vitro immunotoxicity of organophosphate flame retardants in human THP-1-derived macrophages. *Environmental Science & Technology*, *54*, 8900–8908. https://doi.org/10.1021/acs.est.0c01152

Lin, L., Fang, Z., Lin, H., You, H., Wang, J., Su, Y., Wang, F., & Zhang, Z. Y. (2016). Depletion of Cks1 and Cks2 expression compromises cell proliferation and enhance chemotherapy-induced apoptosis in HepG2 cells. *Oncology Reports*, *35*, 26–32. https://doi.org/10.3892/or.2015.4372

Liu, D., Liu, N. Y., Chen, L. T., Shao, Y., Shi, X. M., & Zhu, D. Y. (2020). Perfluorooctane sulfonate induced toxicity in embryonic stem cell-derived cardiomyocytes via inhibiting autophagy-lysosome pathway. *Toxicology in Vitro*, *69*, 104988. https://doi.org/10.1016/j.tiv.2020.104988

Liu, X., Cai, Y., Wang, Y., Xu, S., Ji, K., & Choi, K. (2019). Effects of tris(1,-3-dichloro-2-propyl) phosphate (TDCPP) and triphenyl phosphate (TPP) on sex-dependent alterations of thyroid hormones in adult zebrafish. *Ecotoxicology and Environmental Safety*, *170*, 25–32. https://doi.org/10.1016/j.ecoenv.2018.11.058

Liu, Y., Vidanes, G., Lin, Y. C., Mori, S., & Siede, W. (2000). Characterization of a Saccharomyces cerevisiae homologue of Schizosaccharomyces pombe Chk1 involved in DNA-damage-induced M-phase arrest. *Molecular and General Genetics*, *262*, 1132–1146. https://doi.org/10.1007/pl00008656

Livak, K. J., & Schmittgen, T. D. (2001). Analysis of relative gene expression data using real-time quantitative PCR and the $2^{-\Delta\Delta CT}$ method. *Methods*, *25*, 402–408. https://doi.org/10.1006/meth.2001.1262

Meng, Q., & Xia, Y. (2011). C-Jun, at the crossroad of the signaling network. *Protein & Cell*, *2*, 889–898. https://doi.org/10.1007/s13238-011-1113-3

Mizushima, N., & Komatsu, M. (2011). Autophagy: Renovation of cells and tissues. *Cell*, *147*, 728–741. https://doi.org/10.1016/j.cell.2011.10.026

Pines, J. (1996). Cell cycle: Reaching for a role for the Cks proteins. *Current Biology*, *6*, 1399–1402. https://doi.org/10.1016/s0960-9822(96)00741-5

Poma, G., Glynn, A., Malarvannan, G., Covaci, A., & Darnerud, P. O. (2017). Dietary intake of phosphorus flame retardants (PFRs) using Swedish food market basket estimations. *Food and Chemical Toxicology*, *100*, 1–7. https://doi.org/10.1016/j.fct.2016.12.011

Pu, H., Wang, X., Su, L., Ma, C., Zhang, Y., Zhang, L., Chen, X., Li, X., Wang, H., Liu, X., & Zhang, J. (2015). Heroin activates ATF3 and CytC via c-Jun N-terminal kinase pathways to mediate neuronal apoptosis. *Medical Science Monitor Basic Research*, *21*, 53–62. https://doi.org/10.12659/MSMBR.893827

Qin, L., Tong, T., Song, Y., Xue, L., Fan, F., & Zhan, Q. (2009). Aurora-a interacts with cyclin B1 and enhances its stability. *Cancer Letters*, *275*, 77–85. https://doi.org/10.1016/j.canlet.2008.10.011

Qiu, Z., Oleinick, N. L., & Zhang, J. (2018). ATR/CHK1 inhibitors and cancer therapy. *Radiotherapy and Oncology*, *126*, 450–464. https://doi.org/10.1016/j.radonc.2017.09.043

Reinhardt, H. C., & Yaffe, M. B. (2009). Kinases that control the cell cycle in response to DNA damage: Chk1, Chk2, and MK2. *Current Opinion in Cell Biology*, *21*, 245–255. https://doi.org/10.1016/j.ceb.2009.01.018

Sabroe, I., Dower, S. K., & Whyte, M. K. B. (2005). The role of toll-like receptors in the regulation of neutrophil migration, activation, and apoptosis. *Clinical Infectious Diseases*, *41*, S421–S426. https://doi.org/10.1086/431992

Schreiber, M., Kolbus, A., Piu, F., Szabowski, A., Möhle-Steinlein, U., Tian, J., Karin, M., Angel, P., & Wagner, E. F. (1999). Control of cell cycle progression by c-Jun is p53 dependent. *Genes & Development*, *13*, 607–619. https://doi.org/10.1101/gad.13.5.607

Shen, D. Y., Zhan, Y. H., Wang, Q. M., Rui, G., & Zhang, Z. M. (2013). Oncogenic potential of cyclin kinase subunit-2 in cholangiocarcinoma. *Liver International*, *33*, 137–148. https://doi.org/10.1111/liv.12014

Slotkin, T. A., Skavicus, S., Stapleton, H. M., & Seidler, F. J. (2017). Brominated and organophosphate flame retardants target different neurodevelopmental stages, characterized with embryonic neural stem cells and neuronotypic PC12 cells. *Toxicology*, *390*, 32–42. https://doi.org/10.1016/j.tox.2017.08.009

Sundkvist, A. M., Olofsson, U., & Haglund, P. (2010). Organophosphorus flame retardants and plasticizers in marine and fresh water biota and in human milk. *Journal of Environmental Monitoring*, *12*, 943–951. https://doi.org/10.1039/b921910b

van der Veen, I., & de Boer, J. (2012). Phosphorus flame retardants: Properties, production, environmental occurrence, toxicity and analysis. *Chemosphere*, *88*, 1119–1153. https://doi.org/10.1016/j.chemosphere.2012.03.067

Wang, C., Chen, H., Li, H., Yu, J., Wang, X., & Liu, Y. (2020). Review of emerging contaminant tris(1,3-dichloro-2-propyl)phosphate: Environmental occurrence, exposure, and risks to organisms and human health. *Environment International*, *143*, 105946. https://doi.org/10.1016/j.envint.2020.105946

Wang, M., Yang, S., Cai, J., Yan, R., Meng, L., Long, M., & Zhang, Y. (2020). Proteomic analysis using iTRAQ technology reveals the toxic effects of zearalenone on the leydig cells of rats. *Food and Chemical Toxicology*, *141*, 111405. https://doi.org/10.1016/j.fct.2020.111405

Wang, X., Chang, L., Sun, Z., & Zhang, Y. (2010). Comparative proteomic analysis of differentially expressed proteins in the earthworm eisenia fetida during *Escherichia coli* O157:H7 stress. *Journal of Proteome Research*, *9*, 6547–6560. https://doi.org/10.1021/pr1007398

Wang, X. W., Liu, J. F., & Yin, Y. G. (2011). Development of an ultra-high-performance liquid chromatography-tandem mass spectrometry method for high throughput determination of organophosphorus flame retardants in environmental water. *Journal of Chromatography a*, *1218*, 6705–6711. https://doi.org/10.1016/j.chroma.2011.07.067

Wynn, T. A., Chawla, A., & Pollard, J. W. (2013). Macrophage biology in development, homeostasis and disease. *Nature*, *496*, 445–455. https://doi.org/10.1038/nature12034

Xiong, J. (2015). Atg7 in development and disease: Panacea or Pandora's box? *Protein & Cell*, *6*, 722–734. https://doi.org/10.1007/s13238-015-0195-8

Yang, X., Zhang, Y., Lai, W., Xiang, Z., Tu, B., Li, D., Nan, X., Chen, C., Hu, Z., & Fang, Q. (2019). Proteomic profiling of RAW264.7 macrophage cells exposed to graphene oxide: Insights into acute cellular responses. *Nanotoxicology*, *13*, 35–49. https://doi.org/10.1080/17435390.2018.1530389

Yin, H., Han, S., Chen, Y., Wang, Y., Li, D., & Zhu, Q. (2020). T-2 toxin induces oxidative stress, apoptosis and cytoprotective autophagy in chicken hepatocytes. *Toxins*, *12*, 90. https://doi.org/10.3390/toxins12020090

Zhang, P., Zhang, Y., Liu, K., Liu, B., Xu, W., Gao, J., Ding, L., & Tao, L. (2019). Ivermectin induces cell cycle arrest and apoptosis of HeLa cells

via mitochondrial pathway. *Cell Proliferation*, *52*, e12543. https://doi.org/10.1111/cpr.12543

Zhang, W., Wang, R., Giesy, J. P., Li, Y., & Wang, P. (2019). Tris (1,3-dichloro-2-propyl) phosphate treatment induces DNA damage, cell cycle arrest and apoptosis in murine RAW264.7 macrophages. *Journal of Toxicological Sciences*, *44*, 134–144. https://doi.org/10.2131/jts.44.134

Zhang, Y., & Hunter, T. (2014). Roles of Chk1 in cell biology and cancer therapy. *International Journal of Cancer*, *34*, 1013–1023. https://doi.org/10.1002/ijc.28226

Zhang, Y. W., Jones, T. L., Martin, S. E., Caplen, N. J., & Pommier, Y. (2009). Implication of checkpoint kinase-dependent up-regulation of ribonucleotide reductase R2 in DNA damage response. *Journal of Biological Chemistry*, *284*, 18085–18095. https://doi.org/10.1074/jbc.M109.003020

SUPPORTING INFORMATION

Additional supporting information may be found online in the Supporting Information section at the end of this article.